

Soil organic matter formation and loss are mediated by root exudates in a temperate forest

Received: 10 May 2022

Accepted: 14 October 2022

Published online: 28 November 2022

 Check for updates

Nikhil R. Chari^{1,2}✉ & Benton N. Taylor^{1,2}✉

The amount and composition of root exudates—low-molecular-weight carbon compounds released from living plant roots into soil—are expected to shift under global change, and a growing body of work indicates that root exudates have important impacts on stable soil organic matter dynamics. However, most research on exudate effects on soil organic matter uses highly homogenized or artificial soil, leaving major uncertainties in how exudates will influence carbon dynamics in natural, intact soil systems. We used ¹³C-labelled artificial root exudates to examine the effects of exudation rate and type on stable soil organic matter formation and loss in intact forest soil cores collected over a heterogeneous gradient in a temperate hardwood forest. We observed effects of different exudate treatments on stable soil carbon dynamics that overrode native soil heterogeneity, and higher exudation rates enhanced mineral-associated organic matter turnover but not accumulation. Organic and amino acid exudates led to net mineral-associated organic matter accumulation, with amino acids having particularly strong positive effects on microbial biomass. Simple sugars increased mineral-associated organic matter turnover (both formation and loss) but did not alter the size of this pool. Our results suggest that predicted increases in root exudation rates and compositional shifts towards simple sugars under global change may reduce soils' C storage capacity.

The terrestrial carbon (C) sink captures one-third of anthropogenically produced CO₂ (ref. ¹), but rapidly rising concentrations of atmospheric CO₂ raise questions about how plants and soil will interact to sequester C in the future^{2,3}. Root exudates—low-molecular weight organic compounds released from living plant roots into soil—link plant and soil C responses to elevated CO₂ and are likely to have greater immediate effects on stable soil organic matter (SOM) formation and loss than shoot and root litter inputs^{4–6}. Although there is strong evidence that exudation rate and exudate metabolite composition are likely to shift under elevated CO₂ in response to increased plant C fixation^{7–10}, little is known about how different root exudate species and exudation rates will influence SOM formation and loss under ecologically realistic conditions.

Root exudation can lead to both SOM formation and SOM loss, and its net effect on SOM probably depends on a combination of soil environmental properties and properties of the exudate compounds. Due to their low molecular weight, exudates can have immediate effects on long-cycling mineral-associated organic matter (MAOM)^{4,11}, unlike non-soluble plant compounds, which typically must pass through the particulate organic matter (POM) pool and be decomposed before they can affect MAOM dynamics¹².

SOM formation from root exudates can occur via microbial assimilation of exudates and subsequent microbial turnover or by direct sorption of exudates to soil minerals¹³. Bioenergetically favourable exudates such as simple carbohydrates are more likely to form SOM

¹Department of Organismic and Evolutionary Biology, Harvard University, Cambridge, MA, USA. ²Arnold Arboretum of Harvard University, Boston, MA, USA. ✉e-mail: nchari@oeb.harvard.edu; bentontaylor@fas.harvard.edu

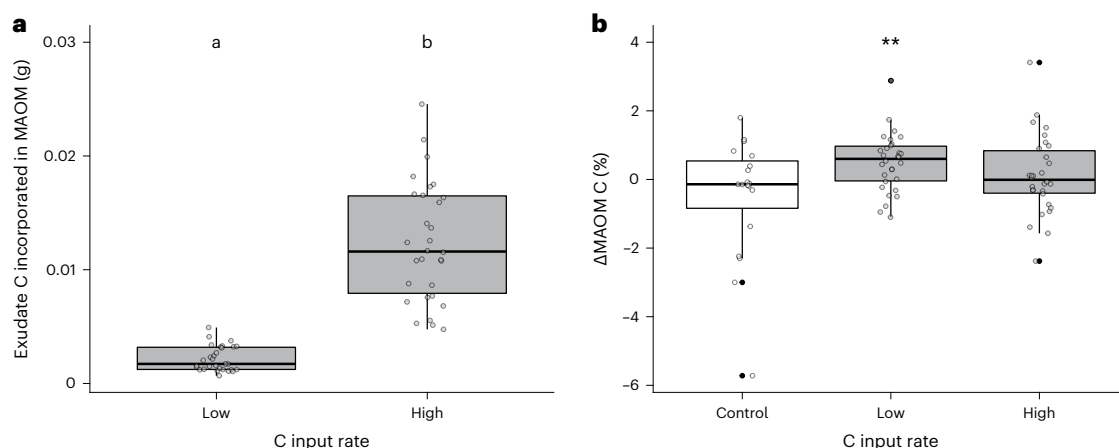


Fig. 1 | Effects of exudation rate on MAOM dynamics. a,b, Effects of exudate C input rate (one-way analysis of variance (ANOVA)) on exudate incorporation into MAOM (**a**) and net change in MAOM between experimental and replicate cores (Δ MAOM) (**b**). In **a**, different letters indicate treatments that are significantly different from one another (one-way ANOVA; $n = 30$; $P_{\text{low-high}} = 5 \times 10^{-15}$). In **b**,

asterisks (*) indicate treatments that are significantly different from the control (one-way ANOVA; $n = 30$; $n = 19$ for control; $P_{\text{ct-low}} = 0.02$). Centre lines for each box represent the median, and the upper and lower limits of the box represent the interquartile range. Error bars represent lower and upper range limits (excluding outliers), and outliers are indicated with bold points.

via microbial turnover¹⁴, while organic acids with reactive carboxylic acid groups may be more likely to sorb directly to soil minerals and form MAOM¹⁵.

Alternatively, root exudates may accelerate C mineralization and SOM loss via the priming effect—fresh C inputs increase microbial activity, stimulating native C mineralization¹⁶. Relatively recent research amends this prevailing theory by suggesting that different root exudate compounds induce the priming effect in different ways¹⁵. Bioenergetically favourable compounds such as Glc appear to stimulate microbial activity via the ‘classic’ priming effect, whereas organic acids with reactive carboxylic acid groups can complex directly with minerals and lead to the dissociation of metal–organic complexes and loss of native MAOM^{11,15}, generally along a gradient of valency¹⁷.

In addition to differences in bioenergetic favourability, nitrogen-(N)-containing root exudate compounds may have unique effects on SOM dynamics given that enhanced C inputs may induce microbial N limitation^{18,19}. Along with carbohydrates and organic acids, N-containing amino acids are frequently released by plants as root exudates^{20,21}. Several studies have shown that Glc (simple sugar) formed more SOM via microbial assimilation than glycine (amino acid), but the specific effect of N was not assayed in these experiments where the different exudate compounds bore little structural similarity to one another^{14,22}. If amino acids alleviate a microbial N limitation, they could suppress priming due to N-mining mechanisms, but N additions that stimulate microbial biomass growth could increase priming overall²³.

Artificial root exudate (ARE) experiments, which pump root exudate-mimicking chemicals into soil systems, are useful for isolating the effects of root exudates on soil C dynamics through experimental manipulation. However, most ARE experiments take place in homogenized or artificial soil systems to make the effects of AREs on soil variables more consistent and easier to observe^{11,15,22,24}. Other experiments have pumped AREs directly into soil in the field^{14,25,26}, but these studies typically occur over smaller spatial areas and incur difficulties when trying to measure change in SOM pools over time.

In this Article, we use a fully factorial ‘best of both worlds’ approach by incubating intact 40 cm³ soil cores representing local variability in soil C (Extended Data Fig. 1) with three different ¹³C-labelled artificial exudate inputs (aspartic acid (AA), succinic acid (SA) and glucose (Glc)) at two different C input rates in a ‘press’ approach over 30 d. In addition, we use structurally analogous organic and amino acid treatments (SA and AA, respectively) to specifically assay the effect of amino N on SOM

formation and loss. Our goal is to observe the individual and interactive effects of (1) root exudation rate and (2) root exudate composition on SOM formation and SOM loss while retaining native soil structure and microbial communities over heterogeneous spatial scales. To measure SOM formation from exudates, we traced ¹³C accumulation in the long-cycling MAOM fraction, and we compared MAOM % C with replicate samples (taken adjacent to each experimental sample but without ARE manipulation) to calculate net MAOM change over the course of the experiment. We measured microbial biomass C (MBC) to determine the effects of different exudate treatments on microbial community size, pore-water ¹³C to assay microbial community turnover and pore-water C to assay SOM priming.

Root exudates influence MAOM dynamics

We found significantly higher ¹³C levels in all treatment samples compared with the control in bulk, MAOM and POM fractions. We found MAOM ¹³C was a better predictor of bulk soil ¹³C ($R^2 = 0.9696$) than POM ¹³C ($R^2 = 0.8451$) and the additive ($R^2 = 0.9694$) and interactive ($R^2 = 0.9690$) effects of MAOM and POM ¹³C, indicating that exudate C inputs influence primarily the long-cycling MAOM fraction. Net change in MAOM C between experimental and replicate cores (Δ MAOM) was significantly affected by both input rate (Fig. 1) and exudate compound type (Fig. 2), but not their interaction. All treatments (including control) showed similar net POM loss (Extended Data Fig. 2) during the experiment, which is expected in the absence of particulate inputs.

Effects of exudation rate

We measured MAOM formation from exudate C by tracing the exudate ¹³C label. As expected, we observed greater MAOM formation from exudate C in the high (35 $\mu\text{mol C cm}^{-2} \text{ d}^{-1}$) than in the low (7 $\mu\text{mol C cm}^{-2} \text{ d}^{-1}$) exudate input treatments (Fig. 1a). After dividing by the amount of exudate C input (to standardize for input rate), high treatments were not significantly different from low treatments, indicating that exudate C was incorporated into MAOM at the same rate per unit input in the low and high treatments. We calculated Δ MAOM between experimental and replicate cores to determine whether MAOM formation from exudate C corresponded with net MAOM accumulation. Despite more exudate C being incorporated into MAOM in the high-rate treatments, Δ MAOM was only significantly higher in the low-rate treatments (Δ MAOM = $+0.49\% \pm 0.85\%$) than the control treatment (Δ MAOM = $-0.50\% \pm 1.77\%$; Fig. 1b). Increases in pore-water C and ¹³C

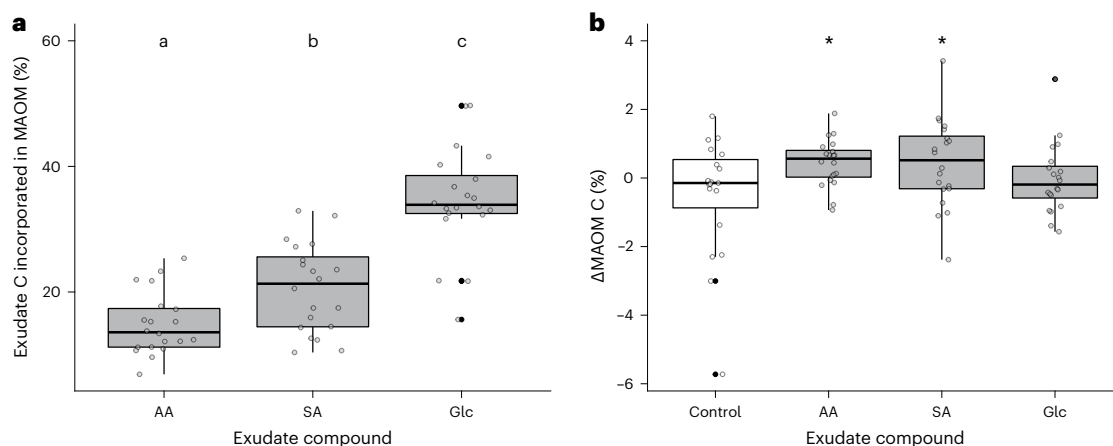


Fig. 2 | Effects of exudate compound type on MAOM dynamics. a, b, Effects of exudate compound type (one-way ANOVA) on exudate incorporation into MAOM (**a**) and net change in MAOM between experimental and replicate cores (Δ MAOM) (**b**). In **a**, different letters indicate treatments that are significantly different from each other ($n = 20$; $P_{AA-SA} = 0.03$, $P_{SA-Glc} = 1 \times 10^{-7}$, $P_{AA-Glc} = 5 \times 10^{-12}$). In **b**, asterisks

(*) indicate treatments that are significantly different from the control ($n = 20$; $n = 19$ for control; $P_{ct-AA} = 0.05$, $P_{ct-SA} = 0.05$). Centre lines for each box represent the median, and the upper and lower limits of the box represent the interquartile range. Error bars represent lower and upper range limits (excluding outliers), and outliers are indicated with bold points.

(indicators of SOM priming and microbial turnover, respectively) were restricted to high-rate treatments (Fig. 3a,b), indicating that both SOM formation and SOM loss are accelerated at high exudation rates.

Effects of exudate type

Our Glc exudate treatments showed the greatest incorporation of exudate C into MAOM ($35\% \pm 8\%$ of total exudate C added; Fig. 2a), but Glc was the only exudate type that did not significantly increase the size of the MAOM C pool (Δ MAOM_{Glc} = $0.04\% \pm 1.00\%$; Δ MAOM_{ct} = $-0.50\% \pm 1.77\%$; Fig. 2b), suggesting enhanced priming may be offsetting enhanced MAOM formation rates in Glc treatments. To confirm this, in the Glc high treatment, we observed elevated pore-water ^{13}C , suggesting rapid microbial uptake of exudate C and microbial turnover (Fig. 3a), and elevated pore-water C, indicating SOM priming (Fig. 3b). In addition, we observed higher levels of pore-water aluminium (Al) and iron (Fe) in Glc high treatments (Extended Data Fig. 3), which indicates that microbes in Glc treatments are priming MAOM specifically by breaking metal–organic bonds^{15,27}, as opposed to POM.

Exudate C incorporation into MAOM was lower in SA treatments than in Glc treatments ($21\% \pm 7\%$; Fig. 2a). However, SA treatments exhibited net MAOM accumulation over the experiment (Δ MAOM_{SA} = $0.44\% \pm 1.29\%$; Fig. 2b). Pore-water ^{13}C was elevated in SA high treatments, suggesting increased microbial turnover (Fig. 3a), but pore-water C was not significantly greater than in the control, suggesting little SOM priming. While SA treatments result in less MAOM formation than Glc treatments, they do not appear to cause a substantial priming effect, resulting in net MAOM accumulation.

Like SA treatments, AA treatments also resulted in net MAOM accumulation (Fig. 2b), despite having the lowest rates of exudate C incorporation into MAOM (Fig. 2a). Low pore-water ^{13}C (Fig. 2a) and increased MBC (Fig. 3c) suggest AA inputs foster microbial community growth with less turnover than Glc or SA inputs. We also observed elevated pore-water C in AA high treatments (Fig. 3b), indicating SOM priming, but lack of pore-water metals and net accumulation of MAOM C suggest AA exudates promote priming of POM, not MAOM. As expected, we also observed significantly greater Δ MAOM N in AA treatments (Extended Data Fig. 4).

Presenting a framework for how root exudates impact SOM

Overall, our results suggest that impacts of exudation rate and composition on SOM in temperate forest soils can be broadly explained by

two principles: (1) increasing exudation rates increasingly favour SOM priming relative to SOM formation (Fig. 4a), and (2) bioenergetically favourable simple sugar exudates increase stable SOM turnover but not net accumulation while amino and organic acids induce lower turnover rates but lead to net accumulation of stable SOM (Fig. 4b).

Root exudates result in stable SOM formation

Our results indicate that SOM formation from root exudates is due largely to MAOM formation via microbial assimilation and turnover. Fossum et al. suggested that MAOM C is derived largely from root exudates;⁴ in this Article, we demonstrate that the inverse of this observation is also true: contributions of root exudates to bulk soil C are driven primarily by contributions to the MAOM C fraction.

Several lines of evidence suggest that exudate–SOM formation pathways are dominated by microbial assimilation rather than direct sorption. First, we found the highest exudate incorporation in Glc treatments, which are more likely than AA and SA to be immediately assimilated by microbes²⁸ (Fig. 2a). In addition, SA and AA have higher direct sorption potential due to the presence of carboxylic acid groups¹⁷, so if direct sorption were the dominant pathway of SOM formation, we would expect higher MAOM ^{13}C signatures in these treatments. However, even in the AA and SA treatments, we observed greater mean increases in Δ MAOM than could be due to exudate C alone. Microbial processing and turnover may have contributed to this excess. Although recent developments in the literature suggest that microbial assimilation may not be the dominant pathway of SOM formation from plant litter^{29,30}, our results suggest exudate–SOM pathways differ from litter–SOM pathways and point to a specific role of exudates in regulating microbial community growth and turnover.

SOM priming offsets formation as exudation rates increase

Although we observed significantly higher exudate incorporation into MAOM at high treatment rates (Fig. 1a), Δ MAOM was significantly greater than the control only in low treatment rates (Fig. 1b). This suggests that MAOM formation is increasingly offset by MAOM priming as exudation rates increase. Accordingly, we observed higher levels of pore-water C, an indicator of priming, in some high-rate treatments but no low-rate treatments (Fig. 3b). In this study, we use pore-water C as a metric of SOM priming as SOM decomposition and release of mineral-bound organics result in enhanced pore-water C levels^{15,31}. We observed differences between patterns of total pore-water C and

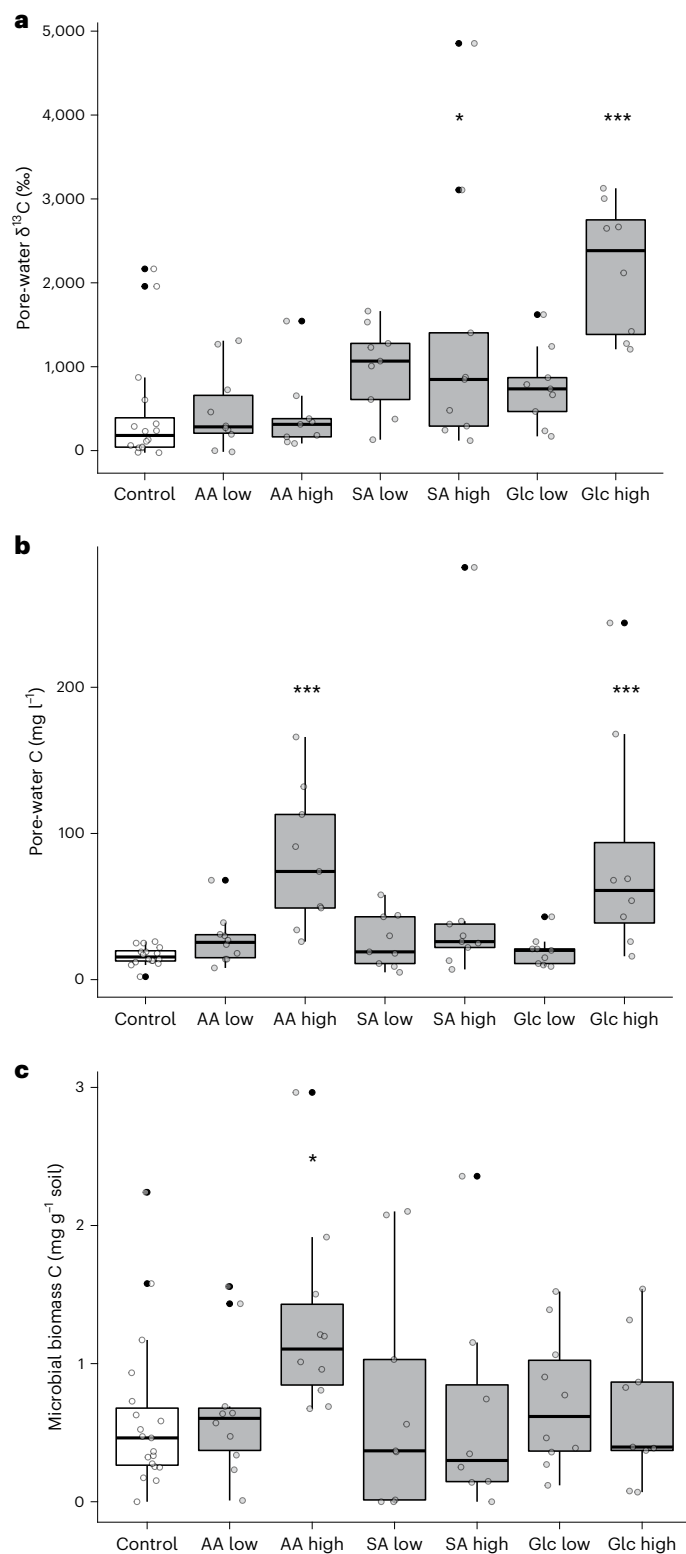


Fig. 3 | Interactive effects of exudate compound type and rate on soil variables. a–c, Interactive effects of exudate compound type and rate (two-way ANOVA; $n = 10$; $n = 19$ for control) on pore-water $\delta^{13}\text{C}$ ($P_{\text{ct-SA high}} = 0.04$, $P_{\text{ct-Glc high}} = 0.001$) (a), total pore-water C ($P_{\text{ct-AA high}} = 0.0001$, $P_{\text{ct-Glc high}} = 0.0001$) (b) and microbial biomass C ($P_{\text{ct-AA high}} = 0.04$) (c). Asterisks (*) indicate treatments that are significantly different from the control ($n = 10$; $n = 19$ for control). Centre lines for each box represent the median, and the upper and lower limits of the box represent the interquartile range. Error bars represent lower and upper range limits (excluding outliers), and outliers are indicated with bold points.

pore-water ^{13}C , which suggest enhanced pore-water C is derived from native MAOM and POM pools rather than exudate C alone (Fig. 3a,b). These results suggest that if exudation rates increase under elevated CO_2 , rates of SOM loss are likely to increase disproportionately to SOM formation, potentially reducing forest soil C storage (Fig. 4a).

Different exudate compounds regulate SOM dynamics through microbes

We observed that AA and SA treatments had significantly higher ΔMAOM than control, indicating net MAOM accumulation over the course of the experiment, while Glc treatments did not (Fig. 2b). This finding is seemingly at odds with highest MAOM ^{13}C in Glc treatments (Fig. 2a). We suggest that Glc is inducing the highest rates of both MAOM formation and MAOM priming (Fig. 4b). While MAOM formation outweighs MAOM priming in AA and SA treatments, these effects offset each other in the Glc treatments.

In the preceding, we suggest that the main pathway of SOM formation from exudates is microbial assimilation and turnover. Pore-water ^{13}C measurements also support this conclusion. We observed elevated pore-water ^{13}C relative to control in Glc high and, to a lesser degree, SA high treatments (Fig. 3a). While some pore-water ^{13}C may be due to experimentally delivered exudate C that is not assimilated by microbes or adsorbed to minerals, we do not believe this is the dominant pathway as Glc has the highest assimilation rate and lowest exogenous residence times of all substrates used in this experiment³². Rather, we suggest that elevated pore-water ^{13}C is due to assimilation of exudate C by microbes and subsequent microbial turnover, which explains why Glc treatments have the highest levels of both pore-water ^{13}C and MAOM ^{13}C (assuming priming and desorption of new exudate-derived MAOM does not vary substantially between exudate treatments).

Contrasting the pore-water C and ^{13}C levels of AA and SA highlights the effect of amino groups on exudate–SOM pathways. Amino groups appear to induce reduced rates of microbial turnover (lower pore-water ^{13}C ; Fig. 3a) and enhanced rates of microbial priming (higher pore-water C; Fig. 3b). Reduced microbial turnover is consistent with lower MAOM formation in AA treatments (Fig. 2a) and elevated MBC in AA high treatments (Fig. 3c). However, enhanced microbial priming is not consistent with higher ΔMAOM levels in AA treatments (Fig. 2b). Thus, we suggest that AA and Glc induce different microbial priming strategies. N inputs in AA treatments may favour microbial community growth (increased MBC) and priming of POM, while Glc treatments may favour a fast-cycling microbial community (no change in MBC but enhanced microbial turnover indicated by elevated pore-water ^{13}C) that is forced to prime MAOM as an N-mining mechanism under C-only inputs^{33,34}. These results are supported by elevated pore-water Al and Fe in Glc high but not AA high treatments (Extended Data Fig. 3), which suggests metal–organic dissociation in Glc but not AA treatments²⁷. Organic acids such as SA appear to result in moderate rates of microbial turnover and low rates of priming. We propose the set of hypotheses in Fig. 4 as one likely explanation for the results observed in this experiment, but stress that further research is needed to interrogate the specific microbially mediated pathways at play.

What is clear is that different exudation regimes have differential effects on SOM dynamics that were detectable despite natural heterogeneity in SOM between our samples (Extended Data Fig. 1). SOM dynamics at Harvard Forest bear similarities to several other temperate forests across the eastern United States and the global average for soil C stocks in cool moist temperate forests^{35,36}. Specifically, we note that McFarlane et al. found a similar proportion of soil C stock in the dense fraction (MAOM) across four temperate forest sites, including Harvard Forest³⁵. Further work is needed to determine how broadly applicable the relationships observed here are in other forest systems.

Organic acids are generally considered the most common category of forest tree root exudates³⁷. Shifts in exudate composition away

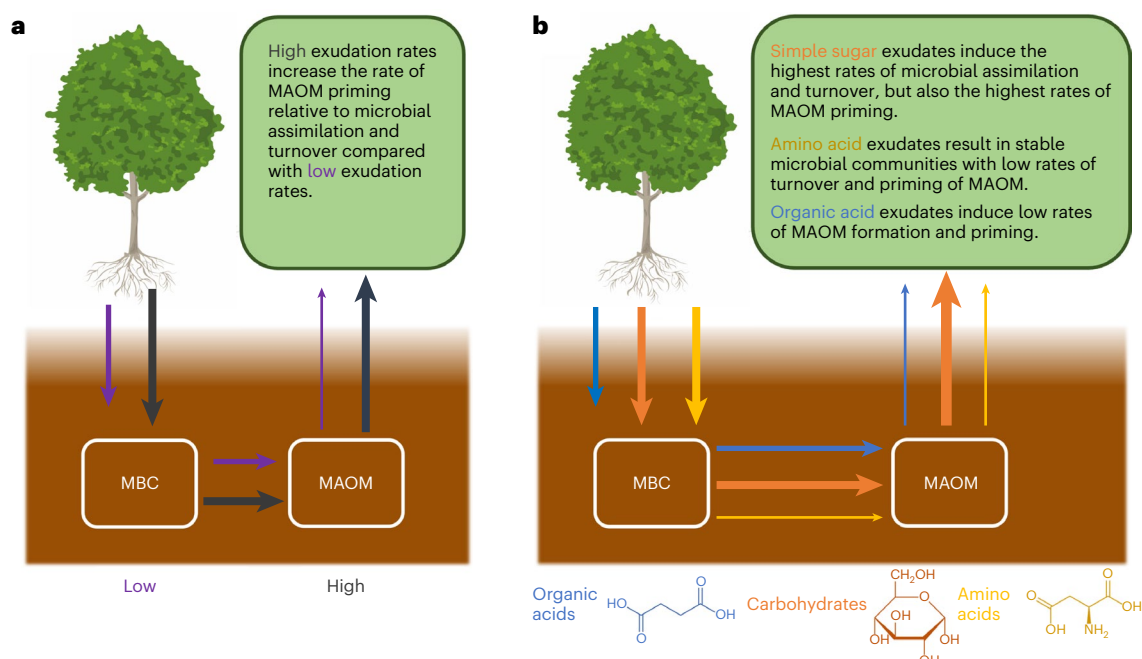


Fig. 4 | Conceptual framework explaining possible roles of exudate compound type and rate in regulating MAOM dynamics. a, b, A conceptual framework to explain the effects of exudation rate (**a**) and exudate type (**b**) on MAOM formation as mediated by microbial assimilation. Moving anticlockwise from the tree, the first set of arrows represents the rate of assimilation of exudate C by soil microbes, the second set of arrows represents the turnover rate of

microbial biomass to MAOM, and the third set of arrows represents the rate of MAOM priming. The width of the arrow represents the size of the C flux. In **a**, purple arrows represent low rates of exudation, and red arrows represent high rates. In **b**, organic acid exudate compounds are represented by blue arrows, simple carbohydrates are represented by orange arrows, and amino acids are represented by yellow arrows.

from organic acids under elevated CO_2 or other climate change drivers could thus increase SOM priming relative to SOM formation⁹, and plants may be incentivized to increase SOM priming as an N-acquisition mechanism in response to increased C fixation¹⁹. We stress that mechanistic effects of different exudate types on pore-water C and ^{13}C were distinguishable only in $5\times$ ambient exudation treatments, which are higher rates than most predictions of elevated CO_2 -induced exudation regimes³⁸. However, our one-month incubation period was short relative to even a single temperate forest growing season³⁹, suggesting that the patterns observed in our study may accumulate over long periods of in situ.

Conclusion

These results provide important evidence for how root exudation drives SOM formation and loss in temperate forests. We find root exudates have an immediate effect on the typically long-cycling MAOM C pool. We find that MAOM formation appears to outweigh MAOM priming, but increasing exudate C concentrations are likely to disproportionately increase rates of priming, potentially leading to SOM loss depending on how elevated CO_2 shifts exudation rates. We also propose differing microbial responses to different exudate treatments, resulting in unique pathways of SOM formation and loss. We suggest bioenergetically favourable simple sugar inputs result in fast-cycling microbial communities, leading to high rates of SOM formation via microbial turnover and high rates of SOM loss via microbial priming. Alternatively, amino acids appear to alleviate microbial N limitation, fostering microbial community growth and moderate priming. These mechanisms further an understanding of how shifts in root exudate composition and rate under climate change will alter long-term soil C sequestration and storage.

Online content

Any methods, additional references, Nature Portfolio reporting summaries, source data, extended data, supplementary information,

acknowledgements, peer review information, details of author contributions and competing interests and statements of data and code availability are available at <https://doi.org/10.1038/s41561-022-01079-x>.

References

1. Keenan, T. F. & Williams, C. A. The terrestrial carbon sink. *Annu. Rev. Environ. Resour.* **43**, 219–243 (2018).
2. Terrer, C. et al. A trade-off between plant and soil carbon storage under elevated CO_2 . *Nature* **591**, 599–603 (2021).
3. Walker, A. P. et al. Integrating the evidence for a terrestrial carbon sink caused by increasing atmospheric CO_2 . *N. Phytol.* **229**, 2413–2445 (2021).
4. Fossum, C. et al. Belowground allocation and dynamics of recently fixed plant carbon in a California annual grassland. *Soil Biol. Biochem.* **165**, 108519 (2022).
5. Rasse, D. P., Rumpel, C. & Dignac, M.-F. Is soil carbon mostly root carbon? Mechanisms for a specific stabilisation. *Plant Soil* **269**, 341–356 (2005).
6. Sokol, N. W., Kuebbing, Sara, E., Karlsen-Ayala, E. & Bradford, M. A. Evidence for the primacy of living root inputs, not root or shoot litter, in forming soil organic carbon. *N. Phytol.* **221**, 233–246 (2019).
7. Calvo, O. C., Franzaring, J., Schmid, I. & Fangmeier, A. Root exudation of carbohydrates and cations from barley in response to drought and elevated CO_2 . *Plant Soil* **438**, 127–142 (2019).
8. Fransson, P. M. A. & Johansson, E. M. Elevated CO_2 and nitrogen influence exudation of soluble organic compounds by ectomycorrhizal root systems. *FEMS Microbiol. Ecol.* **71**, 186–196 (2009).
9. Johansson, E. M., Fransson, P. M. A., Finlay, R. D. & van Hees, P. A. W. Quantitative analysis of soluble exudates produced by ectomycorrhizal roots as a response to ambient and elevated CO_2 . *Soil Biol. Biochem.* **41**, 1111–1116 (2009).

10. Phillips, R. P., Finzi, A. C. & Bernhardt, E. S. Enhanced root exudation induces microbial feedbacks to N cycling in a pine forest under long-term CO₂ fumigation. *Ecol. Lett.* **14**, 187–194 (2011).
11. Jilling, A., Keiluweit, M., Gutknecht, J. L. M. & Grandy, A. S. Priming mechanisms providing plants and microbes access to mineral-associated organic matter. *Soil Biol. Biochem.* **158**, 108265 (2021).
12. Cotrufo, M. F., Wallenstein, M. D., Boot, C. M., Denef, K. & Paul, E. The Microbial Efficiency-Matrix Stabilization (MEMS) framework integrates plant litter decomposition with soil organic matter stabilization: do labile plant inputs form stable soil organic matter? *Glob. Change Biol.* **19**, 988–995 (2013).
13. Sokol, N. W., Sanderman, J. & Bradford, M. A. Pathways of mineral-associated soil organic matter formation: integrating the role of plant carbon source, chemistry, and point of entry. *Glob. Change Biol.* **25**, 12–24 (2019).
14. Bradford, M. A., Keiser, A. D., Davies, C. A., Mersmann, C. A. & Strickland, M. S. Empirical evidence that soil carbon formation from plant inputs is positively related to microbial growth. *Biogeochemistry* **113**, 271–281 (2013).
15. Keiluweit, M. et al. Mineral protection of soil carbon counteracted by root exudates. *Nat. Clim. Change* **5**, 588–595 (2015).
16. Kuzyakov, Y., Friedel, J. K. & Stahr, K. Review of mechanisms and quantification of priming effects. *Soil Biol. Biochem.* **32**, 1485–1498 (2000).
17. Jones, D. L., Dennis, P. G., Owen, A. G. & van Hees, P. A. W. Organic acid behavior in soils—misconceptions and knowledge gaps. *Plant Soil* **248**, 31–41 (2003).
18. Cleveland, C. C. & Liptzin, D. C:N:P stoichiometry in soil: is there a “Redfield ratio” for the microbial biomass? *Biogeochemistry* **85**, 235–252 (2007).
19. Meier, I. C., Finzi, A. C. & Phillips, R. P. Root exudates increase N availability by stimulating microbial turnover of fast-cycling N pools. *Soil Biol. Biochem.* **106**, 119–128 (2017).
20. Canarini, A., Kaiser, C., Merchant, A., Richter, A. & Wanek, W. Root exudation of primary metabolites: mechanisms and their roles in plant responses to environmental stimuli. *Front. Plant Sci.* **10**, 157 (2019).
21. Koo, B.-J., Adriano, D. C., Bolan, N. S. & Barton, C. D. in *Encyclopedia of Soils in the Environment* (ed. Hillel, D.) 421–428 (Elsevier, 2005); <https://doi.org/10.1016/B0-12-348530-4/00461-6>
22. Oldfield, E. E., Crowther, T. W. & Bradford, M. A. Substrate identity and amount overwhelm temperature effects on soil carbon formation. *Soil Biol. Biochem.* **124**, 218–226 (2018).
23. Mason-Jones, K., Schmücker, N. & Kuzyakov, Y. Contrasting effects of organic and mineral nitrogen challenge the N-mining hypothesis for soil organic matter priming. *Soil Biol. Biochem.* **124**, 38–46 (2018).
24. Sokol, N. W. & Bradford, M. A. Microbial formation of stable soil carbon is more efficient from belowground than aboveground input. *Nat. Geosci.* **12**, 46–53 (2019).
25. Drake, J. E. et al. Stoichiometry constrains microbial response to root exudation—insights from a model and a field experiment in a temperate forest. *Biogeosciences* **10**, 821–838 (2013).
26. Falchini, L., Naumova, N., Kuikman, P. J., Bloem, J. & Nannipieri, P. CO₂ evolution and denaturing gradient gel electrophoresis profiles of bacterial communities in soil following addition of low molecular weight substrates to simulate root exudation. *Soil Biol. Biochem.* **35**, 775–782 (2003).
27. Rasmussen, C., Southard, R. J. & Horwath, W. R. Soil mineralogy affects conifer forest soil carbon source utilization and microbial priming. *Soil Sci. Soc. Am. J.* **71**, 1141–1150 (2007).
28. Frey, S. D., Lee, J., Melillo, J. M. & Six, J. The temperature response of soil microbial efficiency and its feedback to climate. *Nat. Clim. Change* **3**, 395–398 (2013).
29. Angst, G., Mueller, K. E., Nierop, K. G. J. & Simpson, M. J. Plant- or microbial-derived? A review on the molecular composition of stabilized soil organic matter. *Soil Biol. Biochem.* **156**, 108189 (2021).
30. Craig, M. E. et al. Fast-decaying plant litter enhances soil carbon in temperate forests but not through microbial physiological traits. *Nat. Commun.* **13**, 1229 (2022).
31. Blagodatsky, S., Blagodatskaya, E., Yuyukina, T. & Kuzyakov, Y. Model of apparent and real priming effects: linking microbial activity with soil organic matter decomposition. *Soil Biol. Biochem.* **42**, 1275–1283 (2010).
32. Hill, P. W., Farrar, J. F. & Jones, D. L. Decoupling of microbial glucose uptake and mineralization in soil. *Soil Biol. Biochem.* **40**, 616–624 (2008).
33. Asmar, F., Eiland, F. & Nielsen, N. E. Interrelationship between extracellular enzyme activity, ATP content, total counts of bacteria and CO₂ evolution. *Biol. Fertil. Soils* **14**, 288–292 (1992).
34. Fontaine, S., Mariotti, A. & Abbadie, L. The priming effect of organic matter: a question of microbial competition? *Soil Biol. Biochem.* **35**, 837–843 (2003).
35. McFarlane, K. J. et al. Comparison of soil organic matter dynamics at five temperate deciduous forests with physical fractionation and radiocarbon measurements. *Biogeochemistry* **112**, 457–476 (2013).
36. Post, W. M., Emanuel, W. R., Zinke, P. J. & Stangenberger, A. G. Soil carbon pools and world life zones. *Nature* **298**, 156–159 (1982).
37. Smith, W. H. Character and significance of forest tree root exudates. *Ecology* **57**, 324–331 (1976).
38. Dong, J. et al. Impacts of elevated CO₂ on plant resistance to nutrient deficiency and toxic ions via root exudates: a review. *Sci. Total Environ.* **754**, 142434 (2021).
39. White, M. A., Running, S. W. & Thornton, P. E. The impact of growing-season length variability on carbon assimilation and evapotranspiration over 88 years in the eastern US deciduous forest. *Int. J. Biometeorol.* **42**, 139–145 (1999).

Publisher's note Springer Nature remains neutral with regard to jurisdictional claims in published maps and institutional affiliations.

Springer Nature or its licensor (e.g. a society or other partner) holds exclusive rights to this article under a publishing agreement with the author(s) or other rightsholder(s); author self-archiving of the accepted manuscript version of this article is solely governed by the terms of such publishing agreement and applicable law.

© The Author(s), under exclusive licence to Springer Nature Limited 2022

Methods

Field sampling

Soils were collected from the Harvard Forest Barre Woods site (42.5° N, 72.2° W). The ecosystem is a temperate mixed hardwood forest characterized primarily by deciduous tree species (specifically *Acer rubrum* and *Quercus rubra*), and the soils are best characterized as Typic Dystrachrepts⁴⁰. Mean annual temperature is 7.5 °C and mean annual precipitation is 1,119 mm yr⁻¹⁴⁰. Bulk soil C from Harvard Forest at 0–5 cm has previously been measured at approximately 10% C with a $\delta^{13}\text{C}$ value of -27‰ (ref.³⁵).

Two replicate soil cores of approximately 8 cm depth and 2.5 cm diameter (~40 cm³ volume, henceforth referred to as ‘experimental’ and ‘replicate’ cores) were taken from 79 randomly distributed locations along a 174 ft perimeter directly outside the control plot of the Barre Woods site on 11 March 2021. Intact experimental cores were placed directly into incubation chambers made from 50 ml centrifuge tubes, each of which had five aeration holes drilled into the tube walls beforehand. Replicate cores were used to approximate soil C at each sample location before experimental treatments. These replicate cores were sealed, refrigerated overnight and analysed the day after sampling. While some disturbance to the soil sample is inevitable when using a 2.5 cm diameter soil probe, we transferred samples directly from the probe to the incubation chambers used for the experiment taking care to create as little disturbance to the soil sample as possible.

Experimental design

The experiment followed a fully factorial design with six different treatments (plus a control treatment) and 79 different samples ($n = 10$ for treatments and $n = 19$ for control). Experimental core samples in incubation chambers were randomly distributed across a rectangular array, and a microporous capillary ‘artificial root’ (Rhizon sampler, Rhizosphere Research Products) was inserted fully into each soil core through a hole in the incubation chamber cap. Each artificial root was connected to a 60 ml syringe through which exudate solution was delivered to the samples at a rate of 1 ml d⁻¹ via a manual pump system for 30 d (12 March–10 April 2021).

To assay the effect of exudation rate on SOM dynamics, we included two different C input rates: 7 and 35 $\mu\text{molC cm}^{-2}$ artificial root surface area per day (0.0099 and 0.0495 total gC, respectively). The 7 $\mu\text{molC cm}^{-2} \text{d}^{-1}$ treatment mimicked ambient root exudation levels at peak growing season in a temperate pine forest^{10,19}, adjusted on the basis of fine root surface area per unit volume measurements⁴¹, and the 35 $\mu\text{molC cm}^{-2}$ was 5× ambient root exudation rates. For each input rate, we used three different artificial exudate treatments (Glc, SA and AA; all common root exudate compounds²¹) to assay the effect of exudate type. SA and AA are structurally analogous except for the amino group; thus, differences between SA and AA treatments are a specific consequence of the presence of an N-containing amino group on AA. All exudate solutions were ^{13}C -labelled with a $\delta^{13}\text{C}$ value of +3,000‰.

Soil analyses

Moisture, bulk density and pH were measured on replicate cores the day after sampling. Particle size fractionation was used to separate the replicate samples into MAOM (<54 μm) and POM (54–2,000 μm) according to ref.⁴². In summary, air-dried soils were 2 mm sieved and shaken with a dispersant (sodium hexametaphosphate) and glass beads for 18 h before being passed sequentially through 2 mm and 54 μm sieves to separate MAOM and POM fractions.

Over the course of the 30 d experiment, experimental samples were weighed weekly to account for soil moisture change. Moisture levels were not adjusted other than via the exudate additions, and there was no significant effect of individual treatments on soil moisture throughout the experiment. At the end of the experiment, Rhizon

samplers were acid washed and randomized, and pore water was extracted using the same Rhizon samplers. This method led to higher baseline $\delta^{13}\text{C}$ values in the pore-water samples; however, any treatment effects observed overrode baseline variability. Particle size fractionation was used to separate MAOM and POM fractions in experimental cores at the end of the experiment.

Soil from the replicate MAOM and POM fractions and from the experimental MAOM, POM and bulk fractions were analysed for % C, % N, $\delta^{13}\text{C}$ and $\delta^{15}\text{N}$ using elemental analyzer isotope ratio mass spectrometry (EA-IRMS), and pore-water samples were analysed for % C and $\delta^{13}\text{C}$ using gas chromatography-isotope ratio mass spectrometry (GC-IRMS). Isotopic analyses were carried out at the Yale Analytical and Stable Isotope Center and Cornell Stable Isotope Lab. Exudate incorporation into SOM fractions was calculated using mass balance based on ^{13}C signatures (Supplementary Methods). Changes in MAOM and POM were measured as the difference in MAOM or POM % C between the final experimental cores and the replicate cores. Microbial biomass C was also measured from the experimental samples using the chloroform fumigation method⁴³. In summary, labile soil C was extracted from a subset of each experimental sample using K_2SO_4 , and a second subset was fumigated with chloroform for 5 d before being K_2SO_4 -extracted. Total organic carbon was measured as non-purgeable organic carbon from both extractions on a total-organic-carbon analyser (Shimadzu Scientific Instruments), and MBC was estimated as the difference in non-purgeable organic carbon between fumigated and non-fumigated samples divided by an extraction efficiency factor of 0.4 (ref.⁴⁴). Pore-water Al and Fe were measured using colourimetric reactions^{45,46} and a visible light spectrophotometer (Vernier).

Statistical analyses

All statistical analyses were carried out in R using analysis of variance (ANOVA) models, and data were verified to meet ANOVA model assumptions before analyses. To assay exudate C incorporation into SOM, we modelled the effects of exudation rate and exudate type on ^{13}C signatures in all soil fractions. We modelled change in soil C and N between experimental and replicate cores in MAOM and POM fractions as a function of exudation rate and exudate type to determine the effects of these variables on net changes in SOM. We also modelled the effects of exudation rate and exudate type on pore-water C, Al and Fe as indicators of SOM priming, and pore-water ^{13}C and MBC as indicators of microbial turnover and community size, respectively. When the interaction between exudation rate and exudate type was not significant, we modelled the effects of these variables individually. For several measurements, we transformed the data before analysis to meet ANOVA model assumptions. For MBC, we used a square root Box-Cox power transformation, and for pore-water C, we used a log normalization. For measurements of exudate C incorporation into MAOM via ^{13}C tracing, we compared non-control exudate treatments with one another. For all other measurements, we used a contrast matrix to restrict ANOVA comparisons such that each exudate treatment was compared with the control, but exudate treatments were not compared with each other. We used a simple linear model to determine the relative influences of MAOM ^{13}C , POM ^{13}C and their additive and interactive effects on bulk soil ^{13}C . In all statistics, we assessed significance at an alpha value of 0.05.

Data availability

Data underlying this study can be found at <https://doi.org/10.6084/m9.figshare.21221288> and metadata at <https://doi.org/10.6084/m9.figshare.21221294>.

Code availability

Code for statistics and figure generation can be found at <https://doi.org/10.6084/m9.figshare.21221300>.

References

40. Giasson, M.-A. et al. Soil respiration in a northeastern US temperate forest: a 22-year synthesis. *Ecosphere* **4**, 140 (2013).
41. Mrak, T. et al. Elevated ozone prevents acquisition of available nitrogen due to smaller root surface area in poplar. *Plant Soil* **450**, 585–599 (2020).
42. Cotrufo, M. F., Ranalli, M. G., Haddix, M. L., Six, J. & Lugato, E. Soil carbon storage informed by particulate and mineral-associated organic matter. *Nat. Geosci.* **12**, 989–994 (2019).
43. Brookes, P. C., Landman, A., Pruden, G. & Jenkinson, D. S. Chloroform fumigation and the release of soil nitrogen: a rapid direct extraction method to measure microbial biomass nitrogen in soil. *Soil Biol. Biochem.* **17**, 837–842 (1985).
44. Haney, R. L., Franzluebbers, A. J., Hons, F. M. & Zuberer, D. A. Soil C extracted with water or K₂SO₄: pH effect on determination of microbial biomass. *Can. J. Soil Sci.* **79**, 529–533 (1999).
45. Ahmed, M. J. & Hossain, J. Spectrophotometric determination of aluminium by morin. *Talanta* **42**, 1135–1142 (1995).
46. Viollier, E., Inglett, P. W., Hunter, K., Roychoudhury, A. N. & Van Cappellen, P. The ferrozine method revisited: Fe(II)/Fe(III) determination in natural waters. *Appl. Geochem.* **15**, 785–790 (2000).

Acknowledgements

We thank C. Berlinger and A. Aguilar for help collecting and processing samples, S. Frey and M. Knorr for facilitating our work at the field site and C. Heslop for statistics advice. Thanks to A. Becker (B & B Fabrications) for the help on designing exudate delivery pumps and B. Erkkila (YASIC) for analytical advice. We also thank the Harvard Forest LTER and specifically A. Barker Plotkin and J. Thompson for their ongoing support with this project. N.R.C. was supported by the Harvard Forest LTER Graduate Student Research Award. The land Harvard Forest occupies is the unceded home territory of the Nipmuc People. Centuries of Indigenous stewardship and knowledge helped

shape the ecosystems we study today, and we honour the vital role of Nipmuc community members in shaping these ecosystems into the future. This honouring is an active process that includes co-developing questions and knowledges, promoting Indigenous community self-determination and continuing to build a reciprocal relationship with the Nipmuc that ensures that this land and its life-giving benefits are mutually accessible, affirming and sustaining.

Author contributions

N.R.C. and B.N.T. conceived and designed the project. N.R.C. conducted the experiments and analysed the data. N.R.C. and B.N.T. wrote the manuscript.

Competing interests

The authors declare no competing interests.

Additional information

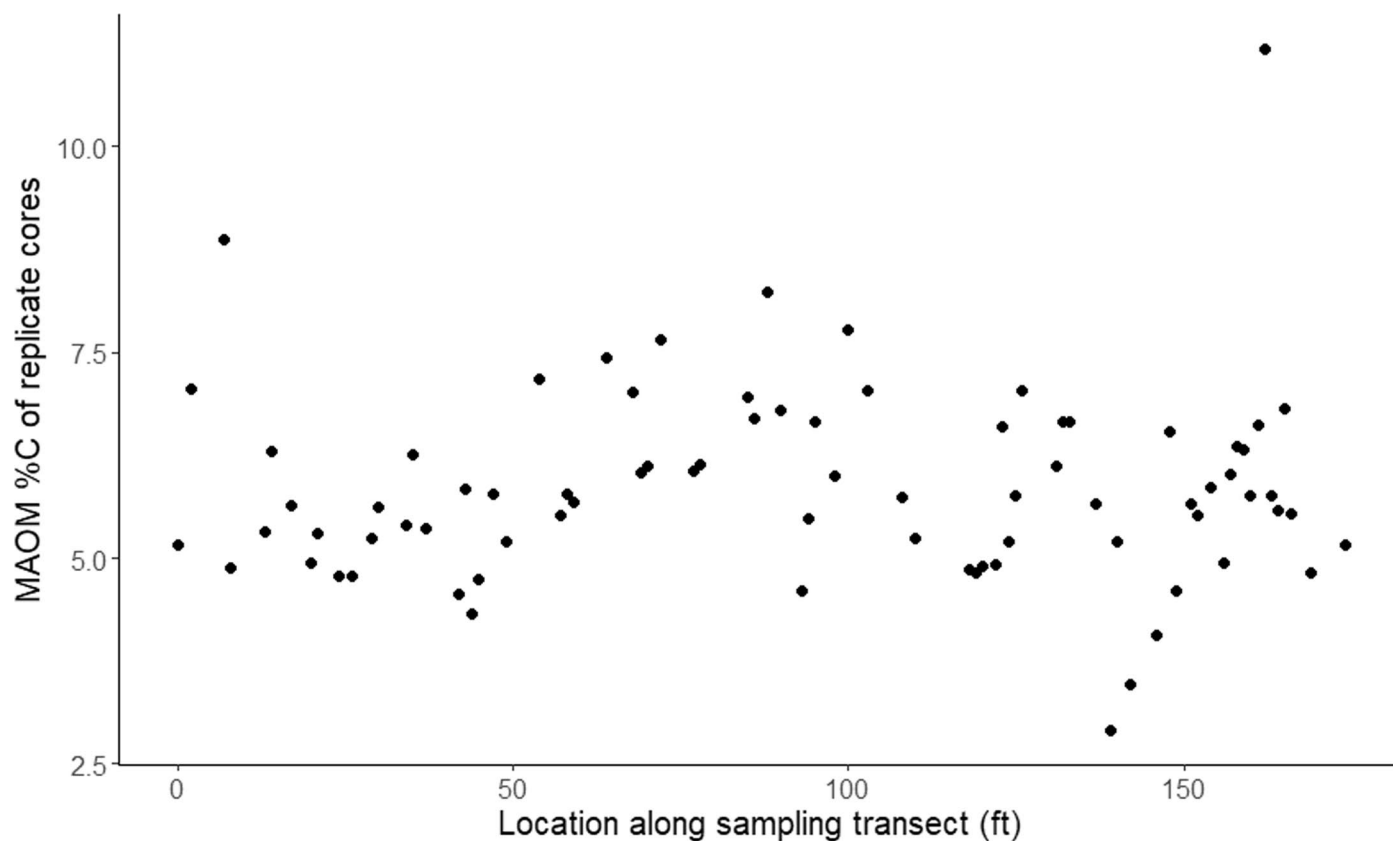
Extended data is available for this paper at <https://doi.org/10.1038/s41561-022-01079-x>.

Supplementary information The online version contains supplementary material available at <https://doi.org/10.1038/s41561-022-01079-x>.

Correspondence and requests for materials should be addressed to Nikhil R. Chari or Benton N. Taylor.

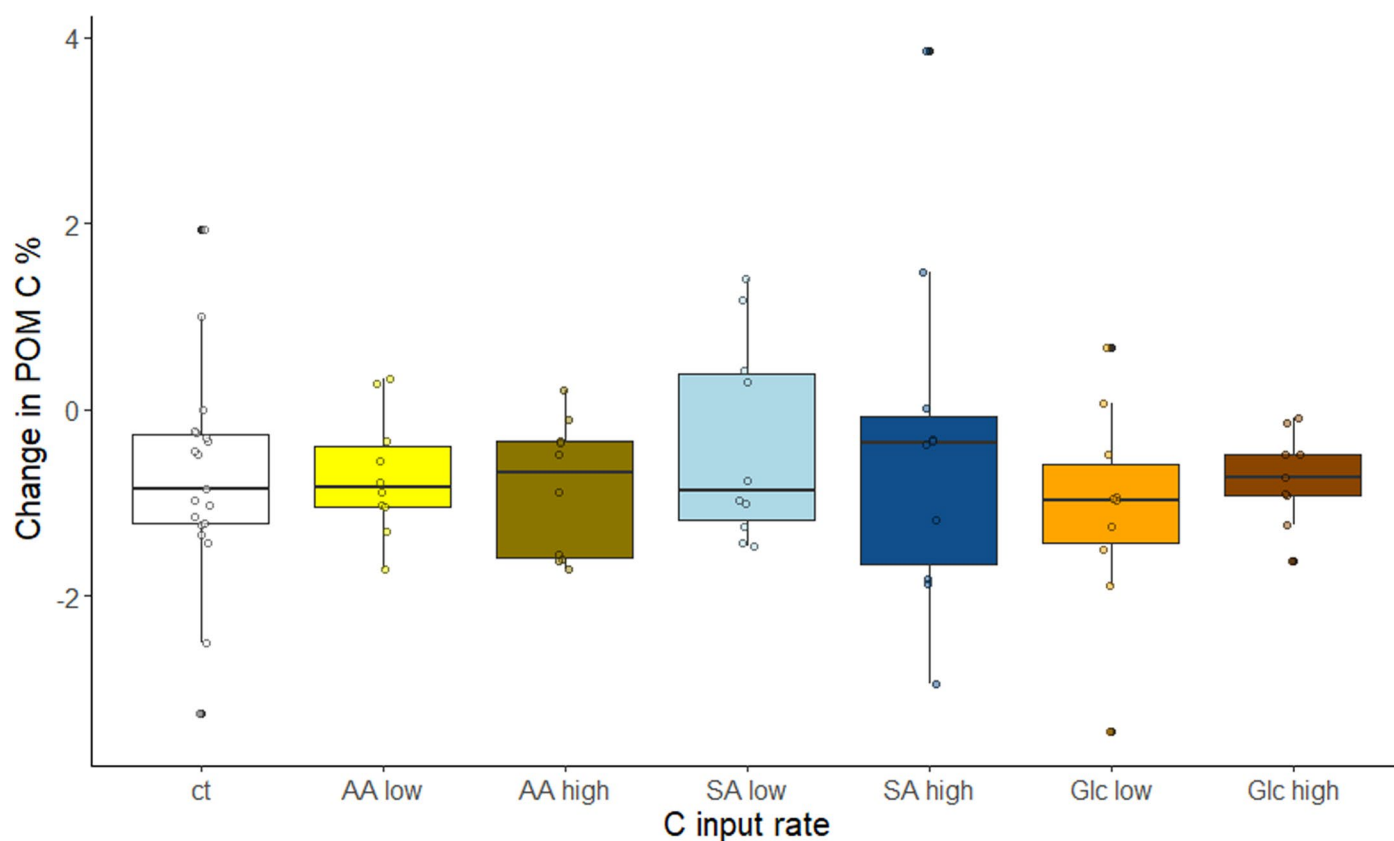
Peer review information *Nature Geoscience* thanks Ashley Keiser and Matthew Craig for their contribution to the peer review of this work. Primary Handling Editor: Xujia Jiang, in collaboration with the *Nature Geoscience* team.

Reprints and permissions information is available at www.nature.com/reprints.



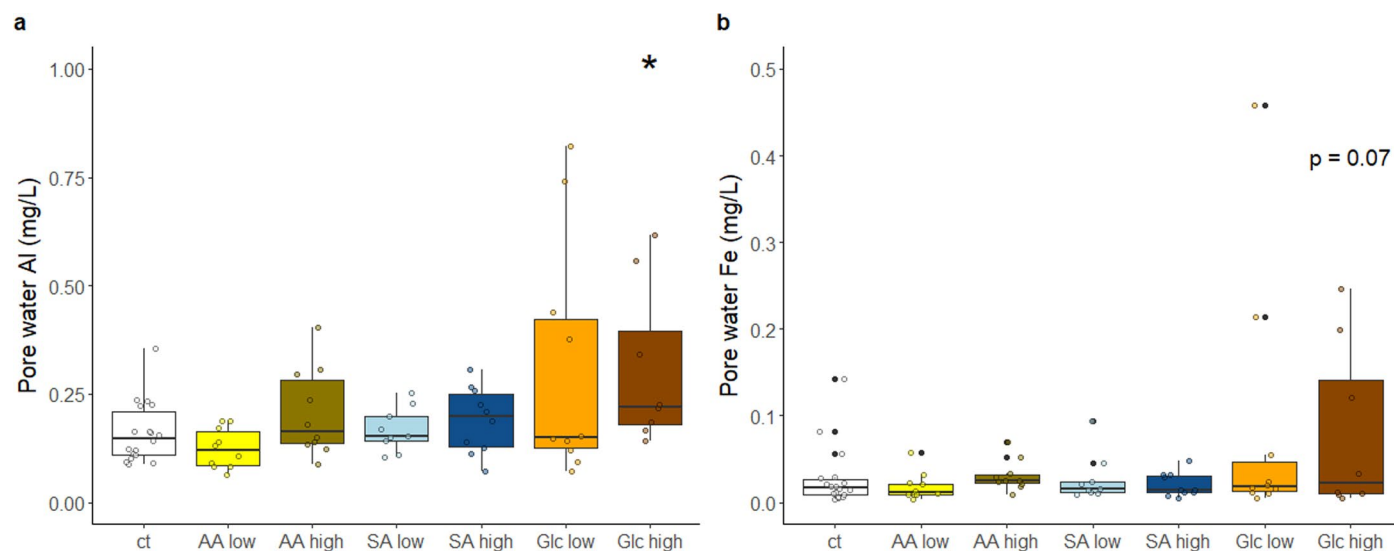
Extended Data Fig. 1 | Variation in MAOM %C of replicate cores across the sampling transect. Each point represents a single replicate core, which were analyzed immediately (1 day) after sampling and did not receive any exudate manipulations. Thus, these data represent natural variation in MAOM %C across

our sampling transect. We note there is fourfold variation in MAOM %C in samples along this gradient. Here, we maintain this heterogeneity in contrast to previous ARE experiments in homogenized soils.



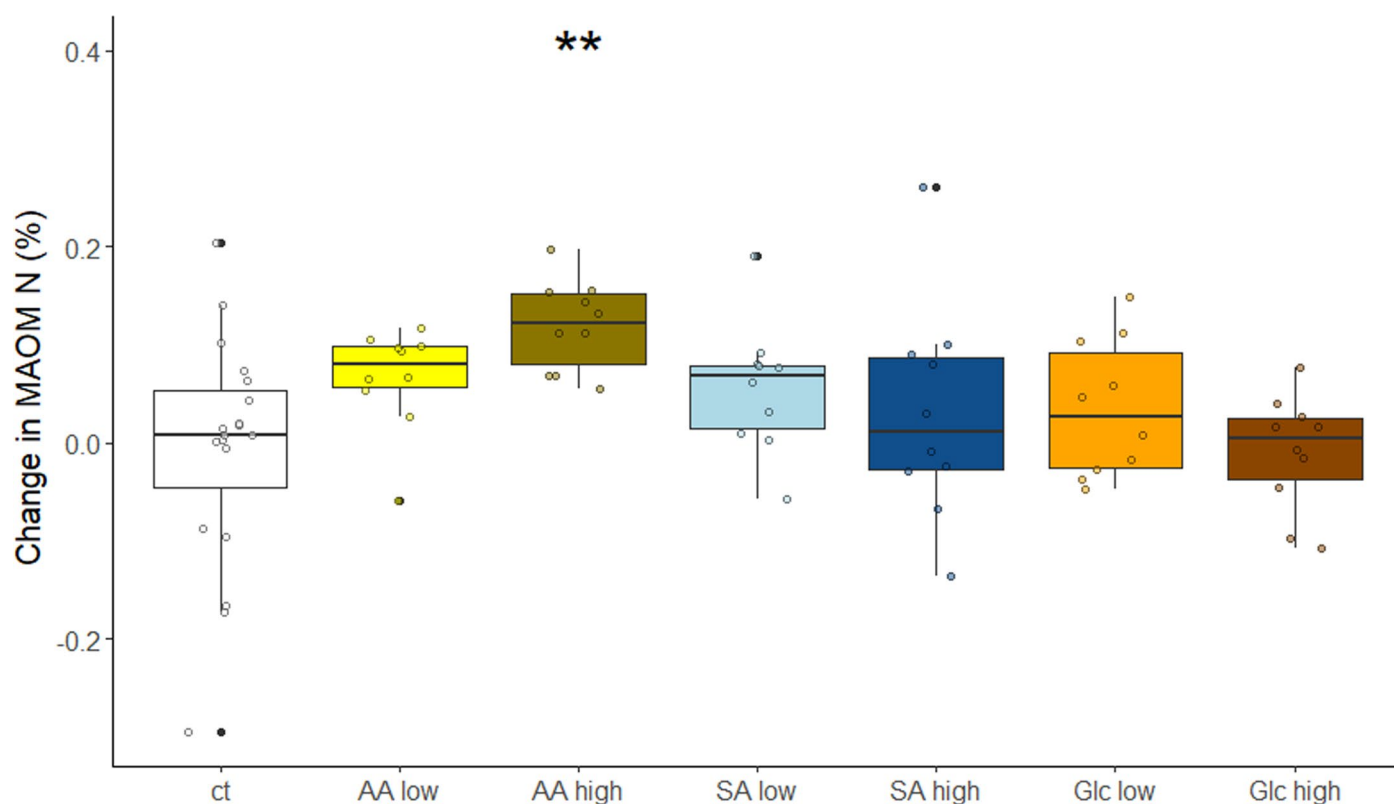
Extended Data Fig. 2 | Change in POM C between experimental and replicate samples (Δ POM) by treatment. All treatments had mean negative Δ POM, indicating POM loss over the course of the experiment. There were no treatment differences from the control under interactive or individual effects of type and rate (ANOVA; $n = 10$, $n = 19$ for control), which may be due to greater

heterogeneity in POM than MAOM pools. Center lines for each box represent the median and the upper and lower limits of the box represent the interquartile range. Whiskers represent lower and upper range limits (excluding outliers), and outliers are indicated with bold points.



Extended Data Fig. 3 | Treatment effects on pore-water metals. Interactive effects of exudate compound type and rate (two-way ANOVA; $n = 10$, $n = 19$ for control) on a) pore-water Al ($p_{\text{ct-Glc high}} = 0.05$) and b) pore-water Fe. Asterisks (*) indicate treatments which are significantly different from the control. Center

lines for each box represent the median and the upper and lower limits of the box represent the interquartile range. Whiskers represent lower and upper range limits (excluding outliers), and outliers are indicated with bold points.



Extended Data Fig. 4 | Change in MAOM N (Δ MAOM N) between experimental and replicate cores. Asterisks (*) indicate treatments which are significantly different from the control (two-way ANOVA; $n = 10$, $n = 19$ for control; $p_{\text{ct-AA high}} = 0.005$). When Δ MAOM N was modelled as a function of exudate type alone, AA

treatments had significantly higher Δ MAOM N than control ($p \leq 0.001$). Center lines for each box represent the median and the upper and lower limits of the box represent the interquartile range. Whiskers represent lower and upper range limits (excluding outliers), and outliers are indicated with bold points.